Scattering of 43-MeV Alpha Particles by the Titanium Isotopes*

J. L. YNTEMA
Argonne National Laboratory, Argonne, Illinois
AND
G. R. SATCHLER
Oak Ridge National Laboratory, Oak Ridge, Tennessee
(Received 17 April 1967)

The elastic and inelastic scattering of 43-MeV α particles on isotopically enriched Ti targets has been measured. The results are analyzed by use of the distorted-wave theory and the collective model. The effect of the choice of different optical-model-potential parameters on the value of the deformation parameter β is investigated and found to be small for reasonable values of the potential parameters. In the three even-A isotopes, a number of 3^- and 4^+ levels have been identified. The excitation mechanisms of the first 2^+ and 4^+ state are compared with the results of coupled-equation calculations and with the predictions of the shell model and the vibrational model.

I. INTRODUCTION

INELASTIC scattering of α particles has been used extensively to obtain information on the excitation of collective states. The elastic scattering of α particles is needed to obtain the optical-model-potential parameters to be used for the distorted-wave analysis of nuclear reactions. Furthermore, a study of the effect of the filling of the $f_{7/2}$ neutron shell on the parameters of the optical-model potential is of interest. The inelastic scattering of α particles has usually been interpreted in terms of the vibrational model. In the case of the titanium isotopes, it was felt that there was sufficient knowledge of the shell-model wave functions to permit a comparison between the predictions of the shell model and the vibrational model. In addition, the motion of the 3^- and 4^+ collective states as neutrons are added to the target nucleus can be followed. Preliminary results on the elastic and inelastic scattering of 43-MeV α particles have been reported previously.[1] The results obtained at Saclay with 42-MeV α particles have been summarized[2] together with an analysis based on the Austern-Blair formalism.

It is well known that there are different families of optical-model-potential parameters that give equally good fits to the experimentally observed angular distributions of elastically scattered α particles. The sensitivity of the deformations obtained from the comparison of experimentally observed inelastic-scattering cross sections and the predictions of different sets of optical-model parameters has been investigated previously[3] for the α-particle scattering from Ni^{58}. In that case the values of β obtained for different sets of parameters were quite similar. The corresponding comparisons have been made in the present experiment, and the sensitivity of the value of β to the use of "best fit" and averaged parameters has been investigated.

II. EXPERIMENTAL PROCEDURE

The experiment was performed in the 60-in. scattering chamber at the Argonne 60-in. cyclotron. The initial experiment was performed with the unanalyzed beam of the cyclotron. The results of this experiment indicated that in many cases adjacent levels were excited. These tended to confuse the measured angular distribution. After the magnetically analyzed beam became available at the cyclotron, it was felt that it would be useful to remeasure the inelastic scattering with an improved resolution. A surface-barrier telescope was used to detect the particles. Its resolution width varied between 135 and 175 keV, depending upon the thickness of the target. The targets were punched out of foils rolled from isotopically enriched material. The isotopic composition of the foils is given in Table I. The inelastic scattering was measured at 2° intervals from 17°–47°. After a

TABLE I. Composition of titanium isotopes (in mole percent).

Target	$\%Ti^{46}$	$\%Ti^{47}$	$\%Ti^{48}$	$\%Ti^{49}$	$\%Ti^{50}$
Ti^{46}	83.8 ±0.1	5.0 ±0.1	9.76±0.08	0.73 ±0.03	0.73 ±0.02
Ti^{47}	1.68 ±0.03	83.05 ±0.08	13.70±0.07	0.798±0.008	0.76 ±0.02
Ti^{48}	0.161±0.002	0.238±0.004	99.08±0.01	0.227±0.006	0.295±0.003
Ti^{49}	1.07 ±0.02	1.27 ±0.05	15.66±0.06	77.2 ±0.3	4.7 ±0.2
Ti^{50}	1.50 ±0.02	1.32 ±0.02	12.2 ±0.1	3.58 ±0.04	81.5 ±0.1

* Work performed under the auspices of the U. S. Atomic Energy Commission.
[1] H. W. Broek and J. L. Yntema, in *Proceedings of the Conference on Direct Interactions and Nuclear Reaction Mechanisms, Padua, Italy, 1962*, edited by E. Clementel and C. Villi (Gordon and Breach Science Publishers, Inc., New York, 1963), p. 769.
[2] G. Bruge, J. C. Faivre, H. Faraggi, G. Valois, A. Brussière, and P. Roussel, Phys. Letters **20**, 293 (1966).
[3] H. W. Broek, J. L. Yntema, B. Buck, and G. R. Satchler, Nucl. Phys. **64**, 259 (1965).

preliminary analysis, it became clear that this angular range and angular spacing was insufficient to determine the optical-model-potential parameters from the experimental data with the required degree of precision. Therefore, the elastic scattering was measured in 1° steps from 10°–51° for the even-even isotopes. Since the enrichment of the isotopes normally was not sufficient to neglect the contamination of Ti^{48}, a computer program was developed to reduce the data to the isotope under consideration. The data were analyzed on the CDC-3600 computer with programs previously described.[4]

III. ELASTIC-SCATTERING RESULTS

The experimental results of the elastic scattering were not corrected for the isotopic contamination in the Ti^{46}, Ti^{48}, and Ti^{50} targets. During the analysis of the data, a Ta contamination in the target gave rise to some uncertainty at small angles. This contamination comes from depositing the Ti on a core of Ta wire in the process of reducing titanium oxide to Ti metal. At the larger angles, the elastic scattering from the heavier element is clearly separated from the elastic scattering from the Ti isotopes, but at the smaller angles this separation could not be made. Therefore, in the analysis it has been assumed that the uncertainty in the data was of the order of 5% except near the minima in the diffraction pattern where an uncertinaty of the order of 8% was assumed. The data were analyzed with an automatic search program written by Perey.[5] It has been shown previously that when the elastic α-scattering data are available for only a limited angular range, it usually is wise to restrict the analysis to a four-parameter potential. While a six-parameter potential may be necessary if the data extend to large angles, this certainly is not true over the limited angular range used in the present experiment. The search program was, therefore, adjusted so that the radius and diffuseness parameters for the imaginary and the real well were the same. It is well known that there are considerable ambiguities in the optical-model-potential parameters that describe the elastic scattering. Consequently, the searches were begun with several different sets of starting parameters in order to obtain different optical-model potentials. Three of the potentials found fit the Ti^{46} elastic-scattering data equally well over the angular range available. The fit of the optical-model potentials to the experimental data is shown in Fig. 1. The real potential-well depth V increases as the radius parameter r_0 decreases, but the product Vr_0^2 for the three potentials is not constant. The diffuseness a decreases slightly with increasing V while the imaginary well depth W increases with V.

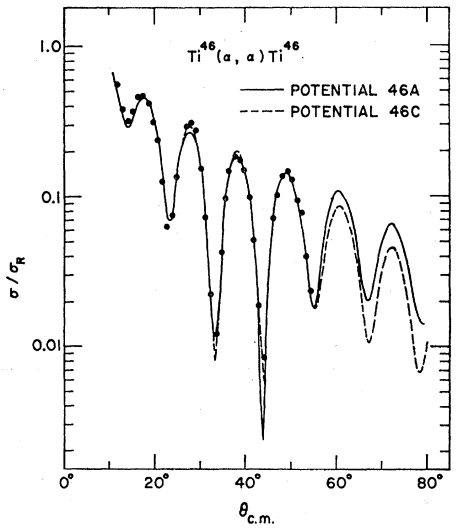

FIG. 1. Elastic scattering of 43-MeV α particles by Ti^{46}.

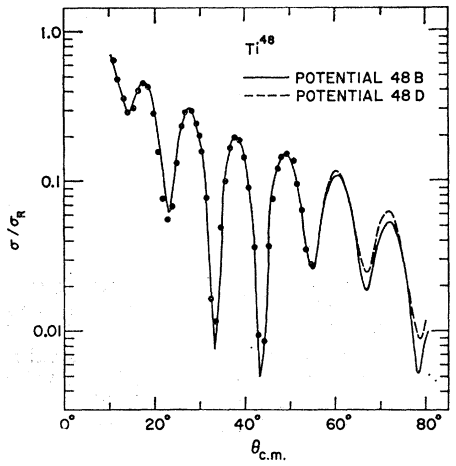

FIG. 2. Elastic scattering of 43-MeV α particles by Ti^{48}.

The three potentials obtained for Ti^{46} were then used as starting guesses to obtain potentials for the Ti^{48} elastic scattering. It was felt desirable to maintain (at least initially) the same value for the radius parameter r_0. Satisfactory potentials were obtained from the two deeper Ti^{46} potentials. Theoretical angular distributions calculated from the two potentials obtained for Ti^{48} with $V \approx 140$ MeV both for the Ti^{46} radius and for the optimum radius are shown in Fig. 2, together with the experimental data. For both $V \approx 183$ and $V \approx 140$ MeV, V is slightly deeper, W is about 10% smaller, and a is somewhat smaller for Ti^{48} than for Ti^{46}. It was not possible to obtain a satisfactory fit to the data with $r_0 = 1.574$ F with $V \approx 70$ MeV. In order to obtain a satisfactory fit with a shallower potential, it is necessary to allow r_0 to vary.

The results obtained for Ti^{48} remain qualitatively true for Ti^{50}. Again a 70-MeV potential with a radius parameter $r_0 = 1.574$ F did not give a satisfactory fit to

[4] H. W. Broek, Argonne National Laboratory Report ANL-6718 (unpublished).

[5] F. Perey (unpublished). We are indebted to Dr. F. G. Perey for making his code available to us.

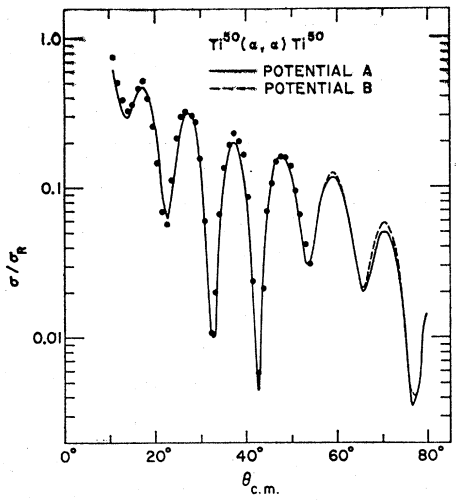

FIG. 3. Elastic scattering of 43-MeV α particles by Ti^{50}.

the angular distribution. However, it was possible to obtain a good fit to the experimental data with the two other types of potential. Here again W is somewhat smaller for Ti^{50} than for either Ti^{46} or Ti^{48}, but the optimum a value is about the same as for Ti^{48}. It is not clear how significant these small changes may be. The angular distributions for Ti^{50} together with the fits obtained for the two deeper potentials is shown in Fig. 3.

IV. INELASTIC SCATTERING

The spectrum of Ti^{46} at 39° lab, corrected for the contamination of the Ti^{48}, is shown in Fig. 4. It is clear that the group near 3.1 MeV contains at least two and possibly three levels. Angular distributions were obtained for the groups at 0.89, 2.00, 3.02, 3.24, 3.55, 3.82, 4.15, 4.72, 5.03, 5.44, and 5.88 MeV.

The spectrum obtained for Ti^{48} at 39° is shown in Fig. 5. Angular distributions for the groups at 0.99, 3.32, 3.81, 4.01, 4.52, 4.89, 5.29, 5.41, 5.50, 5.79, 5.98, and 6.2 MeV have been obtained.

The spectrum obtained from Ti^{50} at 39°, corrected for the contamination of the Ti^{48} in the target, is shown in Fig. 6. Angular distributions were obtained for the states

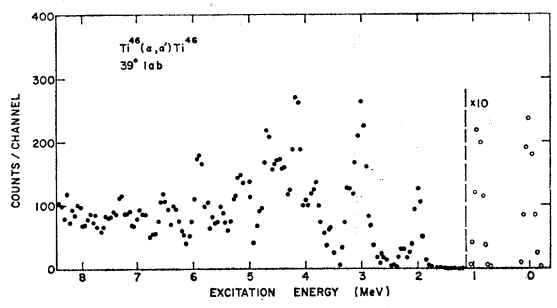

FIG. 4. Spectrum of the scattering of 43-MeV α particles by Ti^{46} at 39°.

at 1.56, 2.66, 4.18, 4.35, 4.76, 5.31, 5.74, 6.5, 6.98, and 7.6 MeV.

Since even the improved resolution of the present experiments was not sufficient to separate the close-lying states in the odd-A titanium isotopes, it was considered to be unnecessary to repeat the experiment on these two isotopes with better resolution.

The data were analyzed by use of the distorted-wave method.[6] It was also considered desirable to investigate how the angular distributions and values of the deformation parameters obtained in the analysis were affected by the use of the different sets of potential parameters and also to investigate the effect of the Ti^{46} potentials for the Ti^{48} and the Ti^{50} isotopes rather than the potentials that best fit the elastic scattering from those nuclei. The excitation of the lowest 2^+ and 4^+ states has

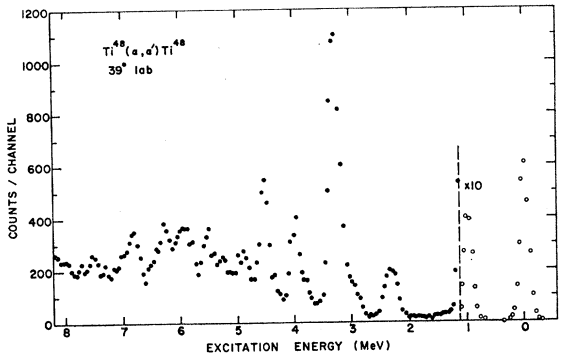

FIG. 5. Spectrum of the scattering of 43-MeV α particles by Ti^{48} at 39°.

been compared with coupled-channel calculations and the results have been summarized earlier and are discussed in more detail in Sec. V. In view of the insensitivity of the predictions to the different optical potentials found in the present work, it was not felt necessary to repeat the analysis previously done with the newer potential parameters (Table II). Of course, other levels can also be reached by multiple excitation processes. However, only in the case of the lowest 4^+

TABLE II. Parameters of the optical-model potential.

Isotope	Potential	V (MeV)	W (MeV)	r_0 (F)	a (F)	r_c (F)	σ/A (mb)	χ^2/N
46	A	69.134	17.79	1.574	0.542	1.4	1455	187
46	B	183.08	28.50	1.438	0.537	1.4	1450	160
46	C	139.22	24.77	1.476	0.540	1.4	1448	165
48	A	186.67	25.96	1.438	0.526	1.4	1462	481
48	B	140.13	22.87	1.476	0.529	1.4	1465	481
48	D	145.88	23.39	1.458	0.540	1.4	1463	377
50	A	182.74	23.43	1.438	0.527	1.5	1489	568
50	B	139.64	20.33	1.476	0.527	1.4	1491	605
All[a]		78.6	15.5	1.576	0.485	1.4	1437	1041

[a] Obtained by optimizing the fit to the earlier elastic data for all the isotopes with $A=46$–50 simultaneously, the scattering angles being scaled according to the diffraction law $\theta'=\theta(A/48)^{1/3}$.

[6] We are indebted to Dr. R. M. Drisko for use of the code JULIE.

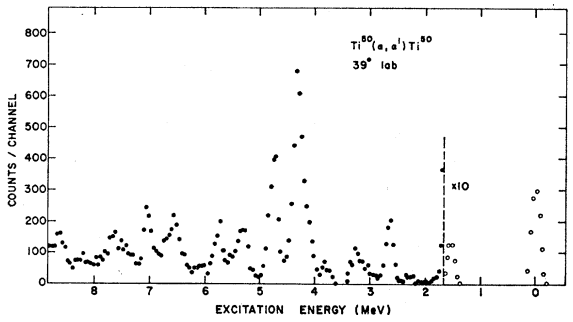

FIG. 6. Spectrum of the scattering of 43-MeV α particles by Ti^{50} at 39°.

levels would such an interaction be at all unambiguous. In the analysis in this section we restrict ourselves to the strong groups that can be assumed to arise from single, direct excitation.

A. Ti^{46} States Above 2 MeV

The angular distribution of the inelastic scattering to states at 3.02, 3.55, and 4.15 MeV is shown in Fig. 7 together with the angular distribution calculated for an $l=3$ transition with potential C for Ti^{46}. The curves obtained from the two other potentials are quite similar to the ones shown here. The agreement between the calculated curves and the experimental data is quite satisfactory. However, the second minima of the 4.15- and 3.02-MeV states are not in quite as good agreement with the calculation as one might have expected. In both cases, this is attributed to the neighboring states which are not completely resolved in the present experiment. The angular distribution of the group observed at 5.88 MeV is shown together with the calculated angular distribution for an $l=3$ transition. In this case the minima are nearly completely filled in. It is unclear whether this is due to the contributions from neighboring states with different angular distributions or to the fact that this is not a one-step $l=3$ transition.

The angular distributions of the groups at 5.03 and 4.72 MeV are also shown in Fig. 7 together with calculated curves for $l=4$ transitions. For the 5.03-MeV data, we have shown the angular distribution for the potential with the real well depth of 183 MeV and have indicated the places where this angular distribution differs from the potential with the well depth of 69 MeV. It is quite clear that the results obtained from these two potentials cannot be distinguished on the basis of the shape of their angular distributions. The angular distribution for the 5.03-MeV state is in good agreement with the calculated $l=4$ angular distribution. The minima appear roughly in the right places for the 4.72-MeV state, but the

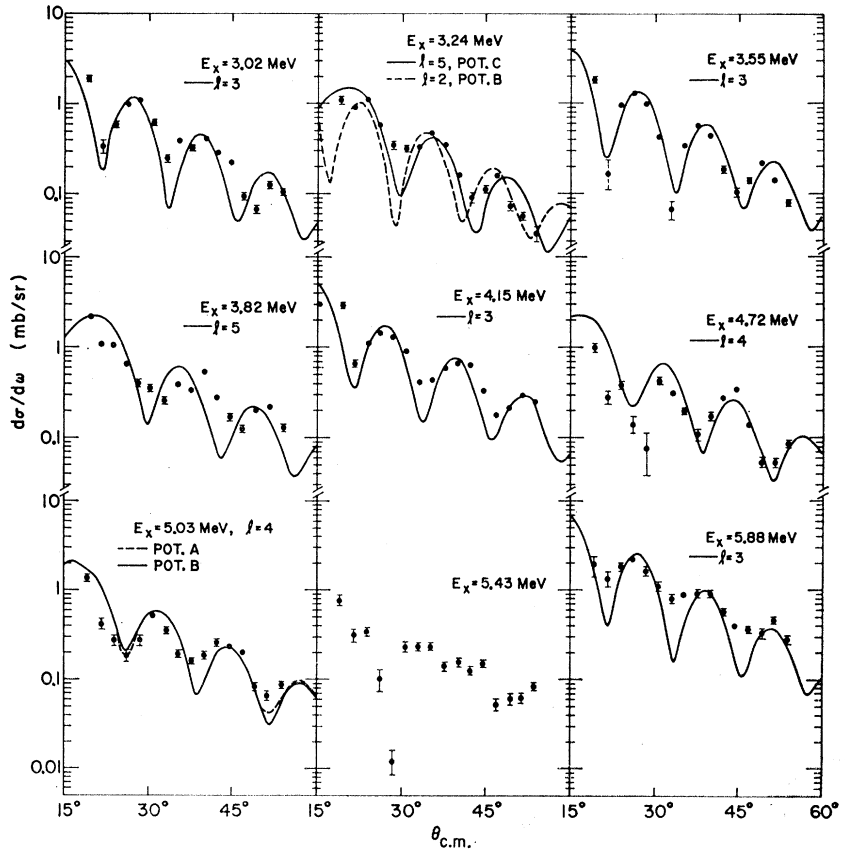

FIG. 7. Angular distributions of a particles inelastically scattered from Ti^{46}. The cross sections have been corercted for isotopic impurity of the target. The curves are the ones obtained from distorted-wave calculations. The potentials used are identified in Table II.

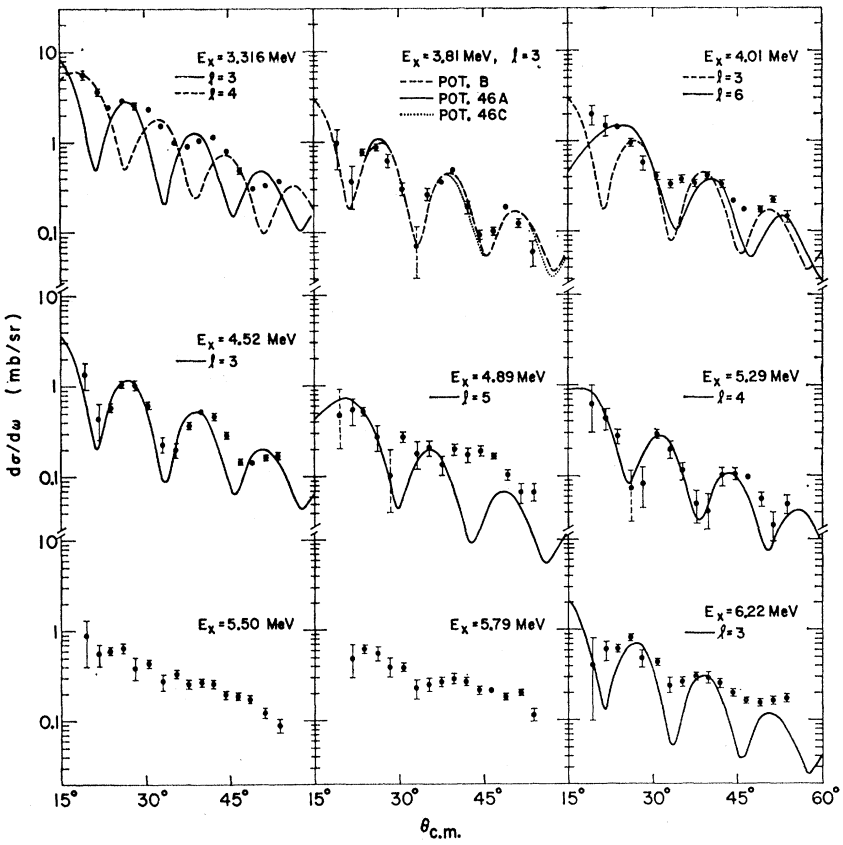

FIG. 8. Angular distributions of α particles inelastically scattered from Ti^{48}. The potentials used for the theoretical curves are identified in Table II.

measured angular distribution does not decrease sufficiently rapidly with increasing angle. The curve shown corresponds to $\beta_4=0.068$. Since the energy of this state is roughly at the sum of the energies of the first 2^+ state and the second or third 3^- state, it is possible that this is an odd-parity level excited at least partly by multiple excitations via the quadrupole and octupole states. It is unlikely that the presence of neighboring states could cause the discrepancy between the calculated and observed angular distributions.

TABLE III. Deformation parameters β.

Isotope	Level energy (MeV)	l	Potential	β
46	0.892	2	A	0.206
46	0.892	2	B	0.229
46	0.892	2	C	0.227
46	3.04	3	B	0.070
46	3.55	3	B	0.080
46	4.15	3	B	0.091
46	5.03	4	A	0.063
46	5.03	4	B	0.070
46	5.03	4	C	0.065
48	0.99	2	B	0.187
48	0.99	2	46 A	0.191
48	0.99	2	46 C	0.193
48	3.813	3	46 A	0.061
48	3.813	3	46 C	0.063
48	3.813	3	B	0.063
48	4.522	3	B	0.068
48	5.29	4	46 C	0.042
50	1.56	2	46 C	0.136
50	2.66	4	B	0.073
50	4.18	4	B	0.083
50	4.35	3	B	0.113
50	4.76	4	B	0.088
50	6.51	3	B	0.066
50	6.98	3	B	0.088
50	7.60	3	B	0.063

The angular distribution of the state observed at 3.82 MeV, together with the predictions for an $l=5$ transition with $\beta_5=0.085$, is also shown in Fig. 7. We do not consider the agreement between the experimental data and the calculated curve to be satisfactory. However, it is clear that more than one level contributes to the measured cross section. The angular distribution for the 3.24-MeV state is shown together with calculated curves for $l=2$ ($\beta_2=0.014$) and $l=5$ ($\beta_5=0.075$). Both curves give equally poor fits to the observed angular distribution. The angular distribution of the 5.43-MeV state shows a very deep minimum near 27° in the center-of-mass system. Since it is impossible to obtain any fit to this angular distribution on the assumption of a one-step direct transition, it seems likely that this level is fed also by multiple excitation.

Table III summarizes the excitation energies and l values for the levels whose identification is reasonably certain, together with the deformation parameters β calculated for the different potentials.

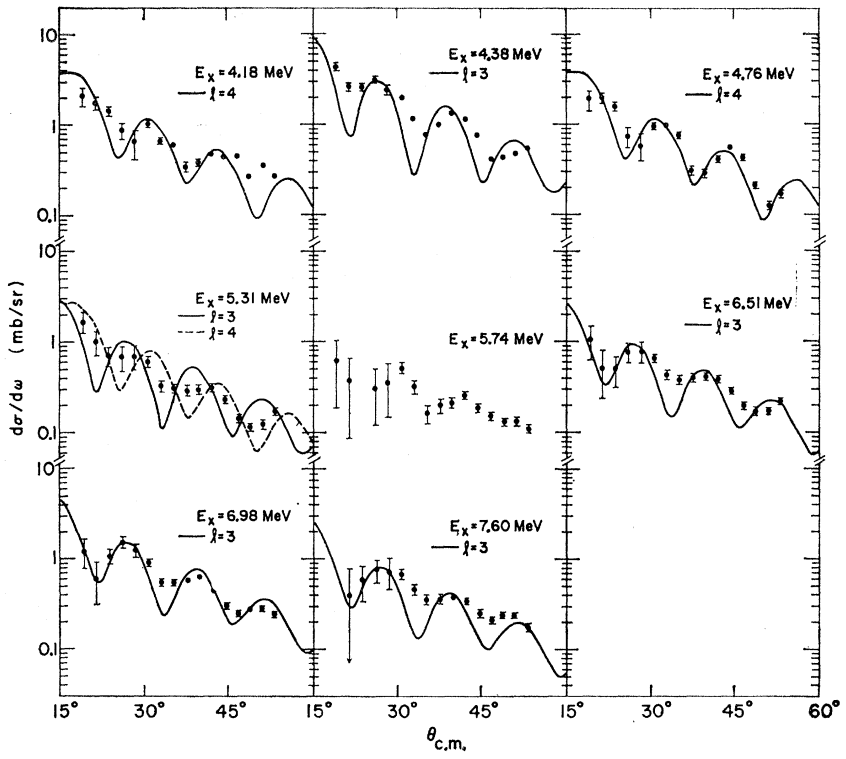

FIG. 9. Angular distributions of a particles inelastically scattered from Ti^{50}.

B. Ti^{48} States Above 3 MeV

The angular distributions of the transitions to the 3.82- and 4.52-MeV 3^- states are shown in Fig. 8, together with the calculated $l=3$ curves. For the 3.81-MeV state, the dashed curve shown was obtained with best fit with a well depth of 140.1 MeV. The deviations from this angular distribution obtained with the Ti^{46} potentials with well depths of 61.1 and 139.2 MeV, respectively, are shown whenever they are significant. The corresponding deformation parameters are included in Table III. Clearly the angular distributions are substantially identical over the range considered, and the β_3 values are very similar. For both levels, the agreement between the theoretical curves and the experimental angular distribution is quite satisfactory.

The angular distribution obtained for the state at 5.29 MeV is shown together with that calculated for an $l=4$ transition. In this case again, excellent agreement between the experiment and calculation is obtained.

The angular distribution obtained for the transition to the group at 3.32 MeV is shown together with the calculated curves for $l=3$ ($\beta_3=0.11$) and $l=4$ ($\beta_4=0.14$) transitions. It is clear that neither curve fits the data. It is possible that more than one state contributes to the measured angular distribution. If so, the two states must be less than 100 keV apart. The angular distributions obtained for the groups at 5.99, 5.79, 5.50, and 4.89 MeV could not be fitted satisfactorily with curves obtained from DWBA (distorted-wave Born-approximation) calculations. The angular distribution of the 5.99-MeV group is quite similar to that of the 5.79-MeV group. For comparison we have shown the calculated $l=5$ ($\beta_5=0.048$) angular distribution together with the 4.89-MeV data. The 4.89-MeV group again occurs approximately at the sum of the first quadrupole and the first octupole excitation energies, but its angular disbution is quite different from that of the 4.7-MeV group in Ti^{46}. The angular distributions calculated for $l=3$ ($\beta_3=0.07$) and $l=6$ ($\beta_6=0.065$) are shown together with the experimental angular distribution at 4.01 MeV. Some semblance of agreement between $l=3$ curve and the experimental data is obtained at angles larger than 25°. However, at forward angles the characteristic minimum for the $l=3$ does not appear. The fit of the $l=6$ curve cannot be considered to be satisfactory either. The angular distribution obtained for the group at 6.2 MeV is shown together with the $l=3$ curve. In this case it is possible that the minima have been filled in by neighboring states. However, it is obvious that the data do not permit the identification of an $l=3$ group at this energy.

C. Ti^{50} Inelastic Scattering Above 3.5 MeV

Figure 9 shows the angular distribution of the 4.38-MeV state together with the calculated $l=3$ curve. The fit of the angular distribution to the experimental data is not quite satisfactory. However, we believe that this is primarily due to the unresolved state at about 4.32

MeV. This state has a different parity and may therefore have filled in the minima in the $l=3$ distribution of the 4.42-MeV state, and also may have shifted our value of the excitation energy somewhat. Other groups with possible $l=3$ angular distributions have been observed at 6.51, 6.98, and 7.6 MeV excitation. The angular distributions for these groups are shown together with the less well developed minima than those calculated, and the agreement is not, perhaps, very satisfactory. The assignments of 3^- to these levels is, therefore, only tentative. Nevertheless, the calculated deformation parameters for these three states are given in the summary in Table III.

The angular distributions obtained for the states at 4.182 and 4.76 MeV are shown together with the calculated $l=4$ curves. The agreement between the 4.76-MeV data and the theoretical curve is quite satisfactory. It is possible that the observed deviations between theory and experiment for the 4.18-MeV group should be ascribed to different spins of the 4.16- and 4.18-MeV levels. Therefore, we have assigned 4^+ to both of these angular distributions. The angular distribution obtained for the 5.74- and 5.31-MeV states are also shown in the figure. The angular distributions for these states cannot be fitted satisfactorily on the assumption of a direct one-step transition. For comparison purposes, the $l=3$ ($\beta_3=0.064$) and $l=4$ ($\beta_4=0.075$) curves have been included with the experimental angular distribution of the 5.31-MeV state.

D. Low-Lying States in Ti^{47} and Ti^{49}

In Ti^{49} only one reasonably sharp group was seen in the initial experiment at an excitation energy of 1.56 MeV. The angular distribution is shown in Fig. 10 together with the distorted-wave curve derived from the last set of parameters in Table II. The angular distribution is clearly an $l=2$ distribution and presumably arises from contributions from the known excited states near this energy.

In Ti^{47}, groups were observed at 1.3, 2.35, 2.67, and 3.0 MeV. The group near 1.3 MeV shows an $l=2$ diffraction pattern, and the group near 2.35 MeV also appears to be fitted rather well with an $l=2$ curve. On the other hand, the 2.67-MeV group is better fitted with an $l=3$ curve, and the group near 3.0 MeV does not show a clear diffraction pattern.

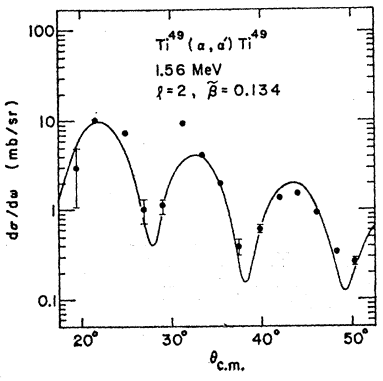

FIG. 10. Angular distribution of the 1.56-MeV α-particle group inelastically scattered from Ti^{49}.

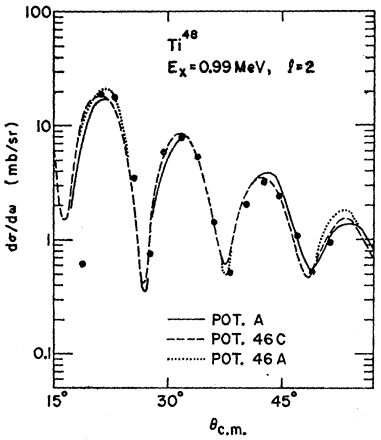

FIG. 11. Comparison of the inelastically scattered α particles from the 0.99-MeV 2^+ level in Ti^{48} and the angular distributions calculated from various optical-model potentials.

V. EXCITATION OF THE LOWEST 2^+ AND 4^+ STATES IN THE EVEN-EVEN ISOTOPES

Let us now consider the first two excited states of the even-even isotopes. It appears of interest at this point to briefly compare the Ti^{48} excitation of the 2^+ state of 0.99 MeV with the calculated angular distributions without the use of the coupled-channel formalism.The experimental angular distribution and three sets of calculated curves are shown in Fig. 11. The dashed curve is the one obtained from Ti^{48} with the potential parameters obtained for Ti^{46} with $V=139$ MeV. The solid line is drawn where the curve obtained with the best-fit potentials at 185 MeV differs markedly from the dashed curve. The dotted curve indicates the deviation from the dashed curve whenever it is significant for the predictions based on the potential obtained for Ti^{46} with a well depth of 69 MeV. The corresponding deformation parameters β_2 are included in Table III. It is clear that neither the calculated angular distributions nor the deformation parameters extracted are sensitive to the fit obtained for the elastic scattering.

In the collective model, the lowest 2^+ level would be regarded as a quadrupole vibration, and the lowest 4^+ state (having approximately twice the energy of the 2^+) would be a member of the triplet of states arising from two quadrupole phonons. Figure 12 compares the data for the 2^+ states with the predictions of the collective model. There is good agreement except that the cross sections observed for the peak at about 20° are somewhat higher than expected. The deformation parameters β_2 are included in Table III. (If the theoretical curves had been normalized to the 20° peak, the values of β

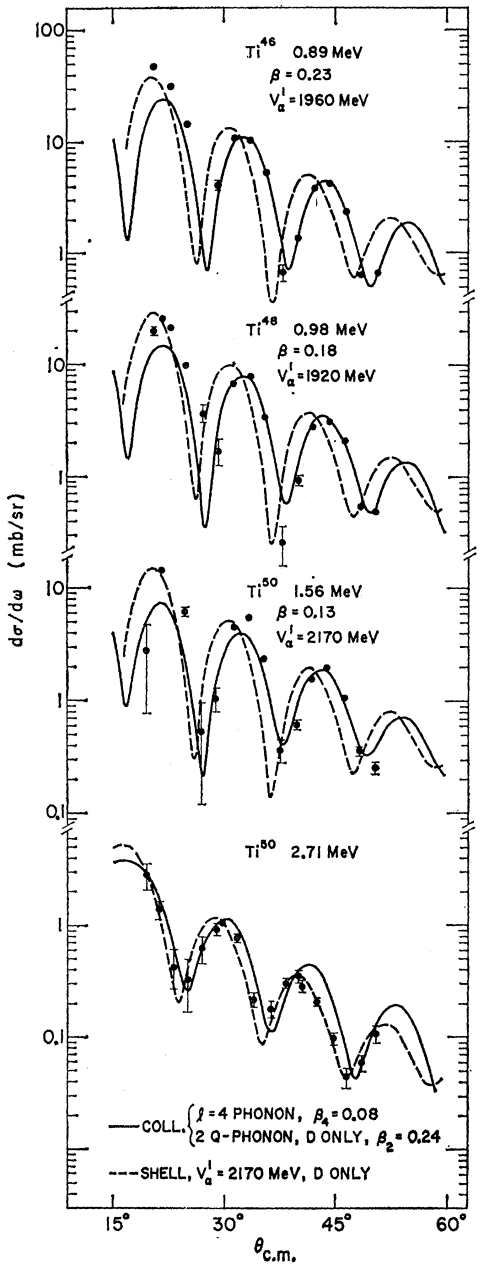

FIG. 12. Comparison between experiment and the predictions of the vibrational model (solid curves) and shell model (dashed curves) for the excitation of the lowest 2^+ states in the even-A isotopes and also the lowest 4^+ in Ti^{50}.

obtained would have been about 20% larger.) The curves shown, and the β_2 values quoted, were obtained by use of optical potentials of Table II with well depth $V \approx 180$ MeV. The results obtained with the other potentials were the same to within a few percent.

The two-quanta vibrational model for the 4^+ states requires the solution of the coupled equations for the ground state and the one-phonon 2^+ and two-phonon 4^+ states, since the vibrational model is known[7] to predict multiple-excitation (in this case, double-excitation) transition amplitudes M which are comparable to the direct $0^+ \rightarrow 4^+$ amplitudes D. However, for values of β of the magnitude encountered here, the vibrational model would predict the same 4^+ angular distributions for all three isotopes. From the data shown in Fig. 13, it is clear that there are marked differences between the isotopes. In particular, the oscillations in the angular distribution for Ti^{48} are almost out of phase with those for the other two isotopes. This kind of change in phase is known[7] to result from changes in the relative impor-

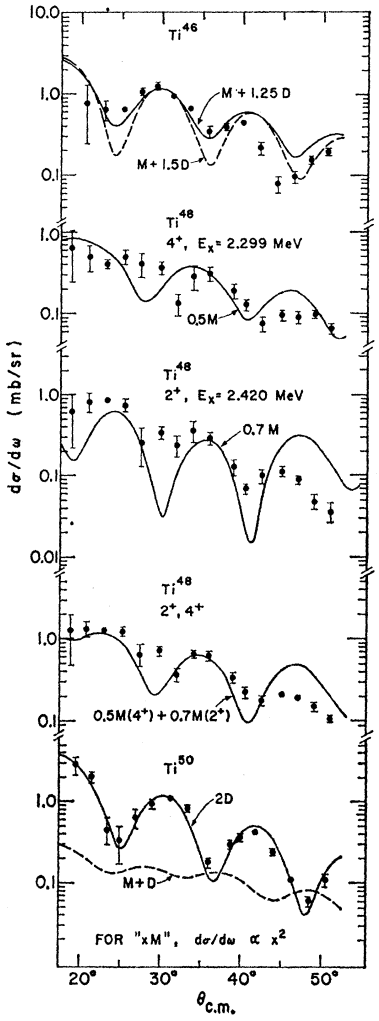

FIG. 13. Comparison of experimental results and theoretical predictions for excitation of the lowest 4^+ states in the even-A Ti isotopes. Collective-model form factors were used, with different weights given to the multiple (M) and direct (D) amplitudes as described in the text. The simple vibrational model would predict nearly the same angular distribution for each target, namely that labeled $M+D$ for Ti^{50}, with a magnitude approximately proportional to β_2^4.

[7] B. Buck, Phys. Rev. 127, 960 (1962); N. Austern, R. M. Drisko, E. Rost, and G. R. Satchler, *ibid.* 128, 733 (1962); T. Tamura, Rev. Mod. Phys. 27, 679 (1965).

tance of the multiple (M) and direct (D) excitation amplitudes. Further, such variations can be expected when the shell structure for these nuclei is taken into account. Their low-lying levels can be accounted for quite well by assuming that the nucleons outside the Ca^{40} core occupy the $1f_{7/2}$ orbit,[8] so that the collective vibrational model could at most be expected to give only a qualitative description of their properties.

A particular prediction of the shell model is that matrix elements of operators of the form

$$\sum_i g_L(r_i) Y_L{}^M(\theta_i\phi_i) \tag{1}$$

will vanish between the ground state and certain excited states of nuclei with j^n configurations that are self-conjugate under interchange of neutron holes and protons.[9] The lowest 4^+ and second 2^+ state in Ti^{48} satisfy these conditions. In the microscopic description of inelastic scattering,[10,11] one pictures the incident α particle interacting with each individual target nucleon so that the interaction operator has the form (1). Then there will be no direct matrix element D coupling the ground state and either of these states in Ti^{48} and hence the transition will have to proceed solely by multiple excitation via other states. The lowest 2^+ will be the dominant intermediate state.

The interaction also depends upon the coordinates (r,θ,ϕ) of the scattered α particle, so that after integrating over the nuclear wave functions the alpha feels an interaction of the form

$$f_L(r) Y_L{}^M(\theta,\phi). \tag{2}$$

The radial shape $f_L(r)$ depends upon the nuclear model used. The collective model[7,12] takes $f_2(r)$ for the $0^+ \rightarrow 2^+$ and $2^+ \rightarrow 4^+$ or $2^+ \rightarrow 2^+$ transitions to be proportional to the first radial derivative of the central optical potential which reproduces the elastic scattering, while $f_4(r)$ for the $0^+ \rightarrow 4^+$ transition and $f_2(r)$ for the transition from the 0^+ to the second 2^+ are proportional to the second radial derivative. The corresponding shell-model form factor is obtained by folding the α-nucleon interaction into the square on the $1f_{7/2}$ radial wave function. However, α-scattering angular distributions are insensitive to the shape of the radial form factor $f_L(r)$ (provided it does not emphasize the nuclear interior excessively) and the magnitudes of the cross sections are determined by the strength of the interaction in the outer regions of the nuclear surface.[12] Hence, for example, multiple excitation ($D=0$) of the 4^+ state in Ti^{48} would be expected to have the same angular distribution whether one used the collective or shell-model prescriptions for the form factor.

These considerations formed the basis of an earlier analysis[13] of these 4^+ cross sections. In that work, the 2^+ and 4^+ states of Ti^{48} were not separated, and their sum was compared with the prediction for the 4^+ state. The present work resovles the two contributions as shown in Fig. 13. The theoretical curves in this figure were obtained from solution of the coupled equations for the interaction (2). The notation used is such that $xM+yD$ denotes that the vibrational-model predictions (normalized to give the observed cross section for the lowest 2^+ state) for the multiple (M) and direct (D) coupling matrix elements have been multiplied by x and y, respectively; $M+D$ then corresponds to the vibrational model itself. The shell-model selection rule predicts M alone ($y=0$) for Ti^{48}; indeed the measured cross sections require predominantly multiple excitation for these states, with a magnitude $x\approx 0.6$.

One can attempt to make this comparison more quantitative by constructing the shell-model form factor (2). This was done[14] by use of the only α-nucleon effective interaction that has proved at all successful so far,[10] namely

$$v(s) = -(V_\alpha/s)(e^{-1.09s} - e^{-1.40s}). \tag{3}$$

The wave function of the target nucleon was calculated for a $1f_{7/2}$ proton bound by 8 MeV in a Woods-Saxon potential well of radius 4.574 F and diffuseness 0.65 F, and subjected to a spin-orbit coupling equal to 25 times the Thomas term. The nuclear matrix elements were computed assuming pure $(f_{7/2})^n$ configurations with no seniority mixing. The resulting cross sections predicted for the 2^+ excitations are shown as dashed curves in Fig. 12, with strengths $V_\alpha = 1960$, 1920, and 2170 MeV for $A=46$, 48, and 50, respectively. The approximate constancy of these V_α shows that the simple configurations assumed do account for the variations in $L=2$ transition strength for these nuclei. The values of V_α are roughly twice those required[10] to explain the 2^+ excitations in Ni^{58} and the Sn isotopes.[15] However, the latter calculations used nuclear wave functions that included considerable correlations. The $E2$ transition strengths for the Ti isotopes require the use of an effective charge of about twice the free proton charge if one assumes pure $f_{7/2}$ configurations, and similar effects may be expected for inelastic scattering. Consequently

[8] J. D. McCullen, B. F. Bayman, and L. Zamick, Phys. Rev. 134, B515 (1964); J. N. Ginnochio and J. B. French, Phys. Letters 7, 137 (1963).

[9] G. T. Garvey, G. M. Crawley, H. O. Funsten, N. R. Roberson, and L. Zamick, Argonne National Laboratory Report No. ANL-6848, 1964, p. 168 (unpublished).

[10] V. A. Madsen and W. Tobocman, Phys. Rev. 139, B8565 (1965).

[11] G. R. Satchler, Nucl. Phys. 77, 481 (1966); and other references given there.

[12] R. H. Bassel, G. R. Satchler, R. M. Drisko, and E. Rost, Phys. Rev. 128, 2708 (1962).

[13] G. R. Satchler, J. L. Yntema, and H. W. Broek, Phys. Letters 12, 55 (1964).

[14] M. B. Johnson and L. W. Owen, Oak Ridge National Laboratory Report ORNL-TM-964, 1964 (unpublished).

[15] N. Baron, R. F. Leonard, John L. Need, W. M. Stewart, and V. A. Madsen, Phys. Rev. 145, 861 (1966).

the present results appear to be roughly consistent with the microscopic analyses for other nuclei.[10,15] The predicted angular distributions in Fig. 12 show similar deficiencies, also. As appears to be a characteristic of this model when applied to α scattering, the predicted oscillations are shifted forward about 5% in angle in comparison both with experiment and with the collective-model predictions.

For the ratio of the coupling matrix element for a $2^+ \rightarrow 4^+$ transition to that for a $0^+ \rightarrow 2^+$, the shell model for Ti^{48} predicts a value which is 0.7 times the prediction from the vibrational model. These ratios are independent of the radial form factors. As Fig. 13 shows, the 0.7 M curve is indeed in good agreement with the data. Further, if we compare the collective and shell-model values of the form factors $f_L(r)$ for radii in the outer part of the nuclear surface, we find that the shell model predicts a direct $0^+ \rightarrow 4^+$ coupling which is several times stronger than that given by the vibrational model, while again the $2^+ \rightarrow 4^+$ coupling is smaller by about the same amount as in Ti^{48}. Hence we would expect a predominantly direct excitation of the 4^+ state in Ti^{50}, and this again is in agreement with the data. The $2D$ curve in Fig. 13 uses twice the collective form factor. With the shell-model form factor and the interaction (3) with the depth $V_\alpha = 2170$ MeV that fits the 2^+ state, the predictions for the direct transition is as shown in the lower part of Fig. 12. The angular distribution shows the same kind of shift as for the 2^+ excitations, but the magnitude is in good agreement with the data. The full curve, shown for comparison, is the distorted-wave prediction of the collective model. (This could be interpreted as for a single 2^4-pole phonon with $\beta_4 = 0.08$ or the direct excitation part of a two-phonon excitation with $\beta_2 = 0.24$. The angular distributions are the same for both cases, despite the quite different form factors involved.)

In Ti^{46}, the shell-model predictions of the ratio of the $2^+ \rightarrow 4^+$ to the $0^+ \rightarrow 2^+$ matrix elements again is less (22%) than the prediction of the collective model. Comparing the values of the form factor shows that the crossover $0^+ \rightarrow 4^+$ amplitude may also be somewhat reduced, so that the shell-model prediction of the ratio of multiple to direct excitation would be close to that given by the vibrational model, but the over-all cross section would be reduced. Figure 13 shows that the data for Ti^{46} are compatible with the vibrational model and that the fit is improved by increasing the direct component. It should be remembered that the shell-model predictions we speak of assumed no seniority mixing. This is unrealistic, and remedying this fault will change the values of the matrix elements.

Finally we should remark that the shell-model cross sections shown in Fig. 12 are virtually independent of the choice of optical potential. Using, for example, the $V \approx 70$ MeV potential with the shell-model form factors yields the same cross sections to within a few percent.

VI. DISCUSSION

A comparison of the values of β extracted with the different sets of potential parameters shows that β is insensitive to the parameters used, provided that these have physically reasonable values. It appears unnecessary to use the "best-fit" parameters for the optical-model potential. Even the last set of parameters listed in Table II, which gives a distinctly poorer fit to the elastic scattering than the others listed, does not affect the value of β by more than 10%. However, the predicted distorted-wave cross section is roughly inversely proportional to the absorptive potential W assumed in the optical potential. Hence the deformation parameter β extracted from a comparison of the experimental and theoretical cross sections is roughly proportional to $W^{1/2}$.

In Ti^{50}, which to a good approximation has a closed $f_{7/2}$ neutron shell and has two $f_{7/2}$ protons outside the closed $d_{3/2}$ shell, we observe a rather strong 3^- state at 4.38 MeV. In the $V^{51}(d,He^3)Ti^{50}$ reaction,[16] the major part of the $s_{1/2}$ hole strength is found in the 4.42-MeV state. This state has also been observed in the $Ti^{49}(d,p)Ti^{50}$ reaction[17] and the inelastic proton scattering[18] from Ti^{50}. The discrepancy in our energy calibration is caused by contributions from the known level at 4.32 MeV which also has contributed to the filling in of the minima of the angular distribution. The 3^- level reported in Ref. 18 is not identified as a 3^- level in the present experiment. The energies of the 3^- levels at 6.51 and 6.98 MeV in Ti^{50} correspond approximately to d-proton hole states. However, not all d-proton hole states are observed in this experiment as states with negative parity. The state near 4.18 MeV contain contributions from both the 4.16- and 4.18-MeV levels. One of these levels is known to contain some admixture of an $f_{7/2}$ proton-hole-state configuration. There is however no known proton hole state corresponding to the 4.76-MeV level. Experimentally some of the observed states in inelastic scattering thus correspond to known proton hole states but one does not observe all of the proton hole states nor are all observed states known as proton hole states. While one appears to see the $s_{1/2}$ and presumed $d_{5/2}$ hole states as 3^- transitions, the presumed $d_{3/2}$-proton hole states are not observed.

In Ti^{48}, which has two neutron holes in the $f_{7/2}$ shell, two low-lying 3^- states are observed with their center of gravity near 4.2 MeV. It is possible that there is a third 3^- state near 3.32 MeV. There is a known 3.23-MeV 4^+ level and 3.34-MeV 6^+ level[19] and it seems likely that both of these levels contribute to the observed group.

[16] B. Zeidman (private communication).
[17] P. D. Barnes, C. K. Bockelman, Ole Hansen, and A. Sperduto, Phys. Rev. **140**, B42 (1965).
[18] W. S. Gray, R. A. Kenefick, and J. J. Kraushaar, Nucl. Phys. **67**, 565 (1965).
[19] P. D. Barnes, C. K. Bockelman, Ole Hansen, and A. Sperduto, Phys. Rev. **138**, B597 (1965).

On the other hand, the cross sections observed for reactions to the 4^+ and 6^+ levels in Ti^{50} together are only about a quarter of the observed cross section for the 3.32-MeV group. On the basis of the cross section and angular distribution, the presence of a third state with spin 3^- in this vicinity does not appear improbable. In Ti^{46} which has four neutron holes in the $f_{7/2}$ shell, three closely spaced 3^- states are observed with the center of gravity near 3.6 MeV, with perhaps a second group at higher excitation energies. It appears that the lowest 3^- strength, which is concentrated in one level in Ti^{50}, is fractionated among two or more levels in the other isotopes—perhaps by interaction with the incomplete neutron shell.

ACKNOWLEDGMENTS

We are indebted to H. W. Broek for his collaboration in the early phases of this experiment and to B. Buck for making available his coupled-equations computer code. The technical assistance of John Bicek and the cooperation of the cyclotron group is gratefully acknowledged.

PHYSICAL REVIEW VOLUME 161, NUMBER 4 20 SEPTEMBER 1967

Study of Analog States by the (p,n) Reaction*

G. P. COUCHELL, D. P. BALAMUTH, R. N. HOROSHKO,† AND G. E. MITCHELL
Columbia University, New York, New York

(Received 27 March 1967)

Isobaric-analog states were studied by measuring the total neutron yield from the (p,n) reaction on ^{65}Cu, ^{70}Zn, ^{74}Ge, ^{76}Ge, ^{75}As, and ^{80}Se. A large number of resonances were observed, and total widths extracted for approximately 50 of these resonances. Detailed comparison is made with the level schemes of nuclei formed by (d,p) reactions on the same targets. Coulomb displacement energies were extracted for all isotopes studied.

INTRODUCTION

ISOBARIC-ANALOG resonances[1,2] have been observed in a variety of nuclei since the discovery of analog states in the compound nucleus by Fox, Moore, and Robson.[3] Methods used include the (p,p), (p,p'), (p,γ), and (p,n) reactions.[4] Measurement of the total neutron yield remains the fastest and simplest way to locate analog states, to measure total widths of these states, and to determine Coulomb displacement energies.

Since the neutron decay of analog states is isospin-forbidden, the observed resonances cannot have pure isospin. The properties of the (p,n) reaction channel are of considerable importance since they give insight into the nature of the mixing between the T-lower states ($T_<=T_t-\frac{1}{2}$; where T_t is the isobaric spin of the target ground state) and T-greater states ($T_>=T_t+\frac{1}{2}$). Measurement of the total neutron yield also serves as a guide to further experiments involving elastic (or inelastic) scattering or detailed neutron studies.

In the present work,[5] the total neutron yield from six intermediate-mass nuclei was measured as a function of incident proton energy. All excitation curves display a number of sharp resonances. A comparison was made between the observed resonances and available level schemes obtained from (d,p) reactions on the same target. In this way many isobaric-analog states of the compound nucleus were identified. Level widths were determined for practically all resonances which were sufficiently well isolated. Coulomb displacement energies were extracted for all isotopes studied, and compared with predictions of a semiempirical formula.

EXPERIMENTAL PROCEDURE

A proton beam was obtained from the Columbia University Van de Graaff accelerator. The relative energy spread of the beam ($\Delta E/E$) was approximately 0.1%. All targets were prepared by evaporation onto 0.010-in. Ta backings. The enrichments of the separated isotopes were: ^{70}Zn(78.3%), ^{74}Ge(91.7%), ^{76}Ge(84.7%), and ^{80}Se(97.75%); natural Cu and As targets were used. Target thickness ranged from 75 to 150 $\mu g/cm^2$, with maximum nonuniformities of 5–10%. The proton beams employed ranged from 0.05 to 0.50 μA. Neutrons were

* Work partially supported by the U. S. Atomic Energy Commission.

† Now at Bartol Research Foundation, Swarthmore, Pennsylvania.

[1] D. Robson, Phys. Rev. **137**, B535 (1965).

[2] C. Mahaux and H. A. Weidenmüller, Nucl. Phys. **89**, 33 (1966).

[3] J. D. Fox, C. F. Moore, and D. Robson, Phys. Rev. Letters **12**, 198 (1964).

[4] *Isobaric Spin in Nuclear Physics*, edited by J. D. Fox and D. Robson (Academic Press Inc., New York, 1966).

[5] A preliminary version of this work was presented at a recent American Physical Society meeting: G. P. Couchell, D. P. Balamuth, R. N. Horoshko, and G. E. Mitchell, Bull. Am. Phys. Soc. **12**, 129 (1967).